Supporting Information

Cnossen et al. 10.1073/pnas.1309438111

SI Text

Investigations in Polycystic Liver Disease-1 Family. ***Ultrasonography.*** Ultrasound images of liver and kidneys were acquired using a 3.6-MHz general purpose clinical echo system (Acuson ×150; Siemens AG) equipped with a curved linear array transducer in all 39 members of proband III/18. Presence or absence of hepatic and/or renal cysts was investigated and noted carefully by at least two clinicians (W.R.C., M.C., and J.P.H.D.). These ultrasound examinations were conducted in all 39 members within 2 wk. During the project, five members (II/13; III/13; III/14; III/21; and III/26) were reevaluated by abdominal ultrasonography (Table S4). Member III/22 could not undergo a second evaluation due to chronic health issues. A complete clinical analysis of the liver and kidney phenotype in these individuals by CT or MRI scanning was not ethically approved for this project.

Ophthalmoscopy. Indirect ophthalmoscopy of the fundus was performed after full mydriasis of the pupil of both eyes by tropicamide 0.5% and phenylephrine 5% (wt/vol) eye drops. By performing slit-lamp biomicroscopy (Kowa SL90 slit lamp and Volk S +70D lens), the posterior and peripheral retina was examined with special attention to the configuration of the retinal vasculature and signs of familial exudative vitreoretinopathy (FEVR). The ophthalmologist (C.E.N.) was ignorant of our whole-exome sequencing results and blinded for this examination in 20 individuals: 11 affected (with *LRP5 c.3562C > T*) and 9 healthy relatives (without *LRP5 c.3562C > T*) in the extended polycystic liver disease PCLD-1 family. These indirect ophthalmoscopy examinations were performed in all 20 members within 1 d.

Laboratory parameters. At the same time, we analyzed metabolic and renal parameters in blood from 22 individuals of this family. All presented values within normal ranges and showed no significant differences between individuals with and without the *LRP5* mutation (Table 2).

Bone densitometry. We assessed bone density of the lumbar spine and left hip by dual-energy X-ray absorptiometry (DXA scan; Hologic Discovery A). Results are reported as T- and Z-scores, which reflect the number of SDs below the average for, respectively, a young adult at peak bone density and an average person of similar age. No relative was known for bone disease, nor was this detected by DXA scanning. The lumbar T-score was lower in *LRP5* mutation carriers, but no relative had a severe bone density disorder. The T- and Z-scores were within the normal-high range: 1.0–2.5 for T-scores and 1.0–2.0 for Z-scores. No significant differences were observed in hip T- and Z-scores and nonpathogenic high-normal values (T- and Z-scores within the normal range, −1.0 to 1.0; Table 2).

Supplementary URLs and Supplementary References for Investigations of PCLD Families. ***URLs.***

- Primer3, v.0.4.0 (latest version): http://frodo.wi.mit.edu/primer3/
- SNP Check, v.3 (latest version); a tool for performing batch checks for the presence of SNPs in predicted PCR primer binding sites: https://secure.ngrl.org.uk/SNPCheck/snpcheck.htm;jsessionid=35D0023CB2F85ABEAAB3FB10C4395F94
- Human genome browser gateway: http://genome-euro.ucsc.edu/cgi-bin/hgGateway?redirect=auto&source=genome.ucsc.edu; v.hg19 human reference genome (GRCh37)
- 1000 Genomes Project, a deep catalog of Human Variation: www.1000genomes.org/data#DataAccess (in 1,000 individuals variants were assessed in the project)
- Exome Variant Server, NHLBI GO Exome Sequencing Project (ESP), Seattle, WA; November 2012 accessed: http://evs.gs.washington.edu/EVS/ (in 6,500 individuals variants were assessed in the project)
- Database of Single Nucleotide Polymorphisms (dbSNP): www.ncbi.nlm.nih.gov/projects/SNP/; Bethesda (MD): National Center for Biotechnology Information, National Library of Medicine; NCBI dbSNP Build 137; 26th June 2012 available
- Mouse Genome Informatics; v.MGI 5.12 (last database update 03–13-2013): www.informatics.jax.org/searches/allele_report.cgi?_Marker_key=37359; MGD
- Human gene mutation database (HGMD Professional) (www.biobase-international.com/hgmd) from BIOBASE Corporation; Professional 2012.4, 14 December 2012 accessed
- MRS database; v.6 (latest version): http://mrs.cmbi.ru.nl/m6/entry?db=sprot&id=lrp5_human&rq=lrp5_human
- The Wnt homepage; 1997–2013 Roel Nusse; last updated June 2013: www.stanford.edu/group/nusselab/cgi-bin/wnt/

References.

Abecasis GR, et al.; 1000 Genomes Project Consortium (2010) A map of human genome variation from population-scale sequencing. *Nature* 467(7319):1061–1073.

Adzhubei IA, et al. (2010) A method and server for predicting damaging missense mutations. *Nat Methods* 7(4):248–249.

Bourhis E, et al. (2011) Wnt antagonists bind through a short peptide to the first β-propeller domain of LRP5/6. *Structure* 19(10):1433–1442.

Chapman AB (2003) Cystic disease in women: Clinical characteristics and medical management. *Adv Ren Replace Ther* 10(1):24–30.

Chen S, et al. (2011) Structural and functional studies of LRP6 ectodomain reveal a platform for Wnt signaling. *Dev Cell* 21(5):848–861.

Cheng Z, et al. (2011) Crystal structures of the extracellular domain of LRP6 and its complex with DKK1. *Nat Struct Mol Biol* 18(11):1204–1210.

Eppig JT, Blake JA, Bult CJ, Kadin JA, Richardson JE; Mouse Genome Database Group (2012) The Mouse Genome Database (MGD): Comprehensive resource for genetics and genomics of the laboratory mouse. *Nucleic Acids Res* 40(Database issue): D881–D886.

Gabow PA, et al. (1990) Risk factors for the development of hepatic cysts in autosomal dominant polycystic kidney disease. *Hepatology* 11(6):1033–1037.

Hoffmann K, Lindner TH (2005) easyLINKAGE-Plus—automated linkage analyses using large-scale SNP data. *Bioinformatics* 21(17):3565–3567.

Hekkelman ML, Vriend G (2005) MRS: A fast and compact retrieval system for biological data. *Nucleic Acids Res* 33(Web Server issue):W766-9.

Kent WJ, et al. (2002) The human genome browser at UCSC. *Genome Res* 12(6):996–1006.

Krieger E, et al. (2009) Improving physical realism, stereochemistry, and side-chain accuracy in homology modeling: Four approaches that performed well in CASP8. *Proteins* 77(Suppl 9): 114–122.

Li B, et al. (2009) Automated inference of molecular mechanisms of disease from amino acid substitutions. *Bioinformatics* 25(21):2744–2750.

Meyer LR, et al. (2013) The UCSC Genome Browser database: Extensions and updates 2013. *Nucleic Acids Res* 41(Database issue):D64–D69.

National Institute of Environmental Health Sciences (2012) Environmental Genome Project Exome Variant Server. Available at http://evs.gs.washington.edu/niehsExome/. Accessed September 28, 2012.

Ng PC, Henikoff S (2003) SIFT: Predicting amino acid changes that affect protein function. *Nucleic Acids Res* 31(13):3812–3814.

Nikopoulos K, et al. (2010) Overview of the mutation spectrum in familial exudative vitreoretinopathy and Norrie disease with identification of 21 novel variants in FZD4, LRP5, and NDP. *Hum Mutat* 31(6):656–666.

Pei Y, et al. (2009) Unified criteria for ultrasonographic diagnosis of ADPKD. *J Am Soc Nephrol* 20(1):205–212.

Ravine D, et al. (1994) Evaluation of ultrasonographic diagnostic criteria for autosomal dominant polycystic kidney disease 1. *Lancet* 343(8901):824–827.

Reynolds DM, et al. (2000) Identification of a locus for autosomal dominant polycystic liver disease, on chromosome 19p13.2-13.1. *Am J Hum Genet* 67(6):1598–1604.

Rozen S, Skaletsky H (2000) Primer3 on the WWW for general users and for biologist programmers. *Methods Mol Biol* 132:365–386.

Sherry ST, et al. (2001) dbSNP: The NCBI database of genetic variation. *Nucleic Acids Res* 29(1):308–311.

Stenson PD, et al. (2009) The Human Gene Mutation Database: 2008 update. *Genome Med* 1(1):13.

Van Keimpema L, et al. (2011) Patients with isolated polycystic liver disease referred to liver centres: Clinical characterization of 137 cases. *Liver Int* 31(1):92–98.

Methodology and Results. ***Luciferase activity assays.*** We performed the luciferase activity assays three times (and in triplicate) in human embryonal kidney cells (HEK293; ATCC CRL-1573). These results were in line with the findings with the CHO cell line for each *LRP5* construct. Both cell lines, HEK293 and CHO, are well-established study models with good transfection efficiencies and applicable to assess functional mechanisms in various disorders (1). Here, we present the results of the luciferase activity assay in transiently transfected HEK293 cells (Fig. S5).

The H69 cells are SV40-transformed normal human liver cholangiocytes originally derived from normal human liver and have been extensively characterized (2, 3). Therefore, we also conducted these experiments in these cells, again three times (and in triplicate), and comparable results were obtained (Fig. S5).

Quantitative PCR experiments. To elucidate the mechanism of *LRP5* mutations in PCLD, we conducted transient transfections of HEK293 cells as previously described. We activated the signaling pathway by addition of Wnt3a for 24 h, similar to former experiments. Expression levels of Wnt target genes *adenomatous polyposis coli* (*APC*), *axis inhibitor-1* (*AXIN-1*), *axis inhibitor-2* (*AXIN-2*), and *glycogen synthase kinase 3β* (*GSK3β*) and *v-myc avian myelocytomatosis viral oncogene homolog* (*c-Myc*), *cyclin D1* (*CCND1*), *lymphoid enhancer-binding factor 1* (*LEF1*), and other target genes were assessed by RNA isolation and subsequently by quantitative PCR (qPCR) experiments (twice in triplicate). These genes are listed at www.stanford.edu/group/nusselab/cgi-bin/wnt/.

Our analyses show that HEK293 cells transfected by mutant *LRP5* led to altered expression levels of target genes compared with WT *LRP5*. Transfected cells expressed LRP5 >5,000 times more. This high number indicates adequate transfection efficiency.

When expression levels for each construct were corrected, there was a significant increased gene expression of APC, GSK3β, c-Myc, and leucine-rich repeat-containing G-protein-coupled receptor 5 (LGR5) in mutant *LRP5*, $LRP5_{R1188W,}$ and $LRP5_{D1551N}$ compared to the WT *LRP5* (Fig. S6). Also, AXIN-1, AXIN-2, CCND1, LEF1, SOX9, Wnt3a, and FGF18 showed increased expression, but this was not significant.

Second, gene expression levels were compared between basal and activated signaling activity by addition of Wnt3a. We corrected activated signaling for basal gene expression for a better understanding of the consequences of mutant *LRP5* on the expression of genes in the up-regulated pathway. Our results indicate unchanged gene expression for APC. Decreased expression levels were found for GSK3β, AXIN-1, AXIN-2, LGR5, and FGF18 compared to WT in both $LRP5_{R1188W}$ and $LRP5_{D1551N}$ (Fig. S7 *A* and *B*).

The same holds true for target genes at the nuclear end point (Fig. S7*C*). CCND1, LEF1, and c-Myc expression levels decreased in mutated *LRP5*. Our results for gene expression levels demonstrate similar effects compared with the luciferase activity assays.

Disease model. Wnt signaling has essential roles in normal tissue development and tumor growth. Wnt signal transduction depends on several proteins interfering with the amount of cadherin binding (at the plasma membrane) and cytoplasmic β-catenin. In absence of extracellular Wnt ligand, the cytoplasmic pool of β-catenin is depleted by the β-catenin destruction complex (proteasome complex) consisting of AXIN, APC, and GSK3β (Fig. S8*A*). The GSK3β phosphorylates sites of the β-catenin and subsequent destruction by ubiquitination and proteolysis is initiated.

Wnt binding activates cytoplasmic Dishevelled (Dsh) to form a signalosome for LRP5 phosphorylation and proteasome destabilization. Subsequently, β-catenin accumulates in the cytoplasm and may be translocated to the nucleus. Binding of β-catenin to Tcf promotes the transcription and expression of Wnt responsive genes (Fig. S8*B*).

We translated our results to this basic scheme of linear canonical Wnt signaling (Fig. S9). We identified no activated signaling by luciferase activity (LEF1/Tcf) assays in mutant *LRP5*. This result resembles our findings from the abovementioned additional experiments. Although the signal transduction is affected in mutant *LRP5*, we hypothesize that the proteasome complex remains active. Second, we hypothesize that a portion of β-catenin accumulates in the cytoplasm, and some β-catenin is destroyed (indicated by a cross with interrupted lines). In addition, it has been proven that β-catenin also binds to cadherins at the plasma membrane in PCLD (4). Therefore, β-catenin does not enter the nucleus to bind Tcf for modulation of expression levels of genes associated with proliferation.

LEF1 is able to activate transcription independently from the presence of β-catenin. We found increased LEF1 expression in mutated *LRP5*, but lower levels compared with WT after addition of Wnt3a. There could be other factors influencing the equilibrium between the membrane and cytoplasmic β-catenin (5). The exact mechanism needs to be explored, and the network of protein interactions in this pathway is major and complex.

In conclusion, in the presence of Wnt3a, signal activation is down-regulated in $LRP5_{R1188W}$ and $LRP5_{D1551N}$.

1. Ai M, Heeger S, Bartels CF, Schelling DK; Osteoporosis-Pseudoglioma Collaborative Group (2005) Clinical and molecular findings in osteoporosis-pseudoglioma syndrome. *Am J Hum Genet* 77(5):741–753.
2. Chen XM, et al. (2005) Multiple TLRs are expressed in human cholangiocytes and mediate host epithelial defense responses to Cryptosporidium parvum via activation of NF-kappaB. *J Immunol* 175(11):7447–7456.
3. Kiel DP, et al. (2007) Genetic variation at the low-density lipoprotein receptor-related protein 5 (LRP5) locus modulates Wnt signaling and the relationship of physical activity with bone mineral density in men. *Bone* 40(3):587–596.
4. Waanders E, Van Krieken JH, Lameris AL, Drenth JP (2008) Disrupted cell adhesion but not proliferation mediates cyst formation in polycystic liver disease. *Mod Pathol* 21(11):1293–1302.
5. Sharpe C, Lawrence N, Martinez Arias A (2001) Wnt signalling: A theme with nuclear variations. *Bioessays* 23(4):311–318.

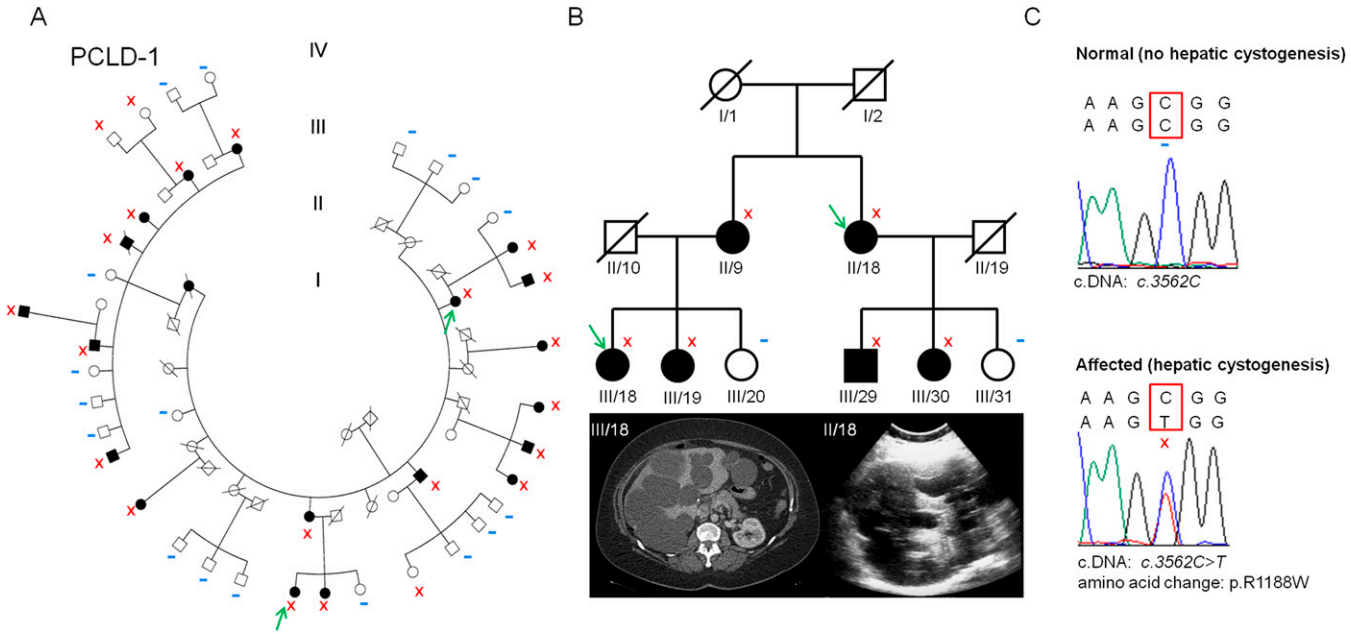

Fig. S1. PCLD-1 family with genotype analysis. This additional figure illustrates the information from Table S4. (*A*) Pedigree of family PCLD-1 presents hepatic and/or renal cystogenesis phenotype ($n = 19$, of which 16 with a polycystic liver) of the 40 members included for analysis (Fig. 1) marked with genotype status (x in red; or - in blue). (*B*) Both affected relatives (II/18 and III/18) are indicated by an arrow (in green) and included for exome sequencing. (*C*) Fig. S1 *A* and *C* indicates which member possessed the heterozygous *LRP5 c.3562C > T* variant (x in red) and individuals with the normal variant (- in blue). Generations are denoted with Roman numerals, and individuals are numbered in a counterclockwise way. Squares indicate male sex, and circles indicate female sex. Solid symbols denote affected individuals, and open symbols are individuals without or unknown for PCLD. A slash indicates that the individual is deceased.

Project:	WYBRICH CNOSSEN	Inheritance:	Dominant
Family name:	TOTALS	Common allele:	99.90 %
Used map:	LDB v2 (sex−averaged)	Disease allele:	0.10 %
Marker positions:	1 ok / 0 ? / 0 outside	LC1 PCOPY rate:	0.00 %
Allele frequencies:	All individuals from marker file	LC1 PENET wt/mt:	80.00 %
CALC interval:	Entire chromosome	LC1 PENET mt/mt:	80.00 %

Marker	CHR	cM	LOD	Theta
1. D11S4117	11	58.00	4.6181	0.0000

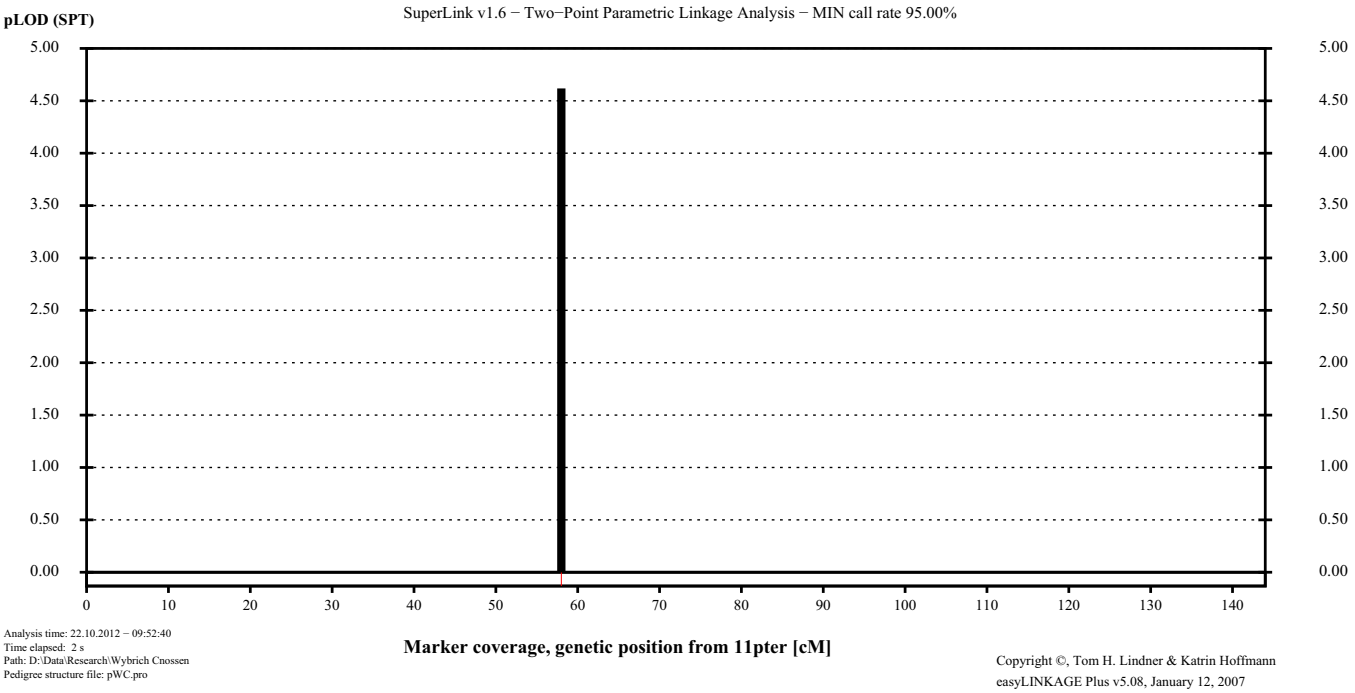

Fig. S2. Logarithm of odds (LOD) score calculation in the PCLD-1 family. The index family (PCLD-1) is a large pedigree segregating *LRP5 c.3562C > T* (p. R1188W). We calculated the LOD score in this family using the FastLink v2.51 program in the EasyLinkage v5.08 software package (8). To determine the actual two-point LOD score for the *LRP5* mutation detected in PCLD-1 family, the mutation was considered to be a microsatellite marker in close proximity of *LRP5* (e. g., D11S4117; Fig. S2). Both for the simulation and the LOD score calculation, an autosomal dominant mode of inheritance was assumed with a penetrance of 0.8 (80%), and the disease allele frequency was estimated at 0.0001. Individuals below the age of 40 (fourth generation; $n = 5$) were not included in this analysis due to the age of onset of the phenotype. We analyzed the sequence data from 35 family members ($n = 18$ members with cystogenesis; $n = 17$ healthy members). Based on the number of individuals with *LRP5 c.3562C > T* ($n = 19$), genome-wide SNP analysis combined with linkage analysis would likely have resulted in a genome-wide significant LOD-score for a genomic region harboring the pathogenic mutation. Because we did not use SNP genotyping, in retrospect, we calculated the highest possible (maximum with $\theta = 0$) LOD score for this family ($n = 35$), which was found to be 7.88. However, nonpenetrance is frequently observed in PCLD, which was supported by the fact that in this index PCLD-1 family, one healthy member and two individuals with bilateral renal (and splenic) cysts, without a hepatic cyst did carry the pathogenic mutation. Taking this into account, we assumed our mutation to be a microsatellite marker and included all family members above the age of 40 y that were genetically tested ($n = 35$). Our analysis resulted in a two-point LOD score of 4.62 that, despite the presence of individuals without a hepatic cyst that carried the mutation ($n = 3$), is considered to be genome-wide significant.

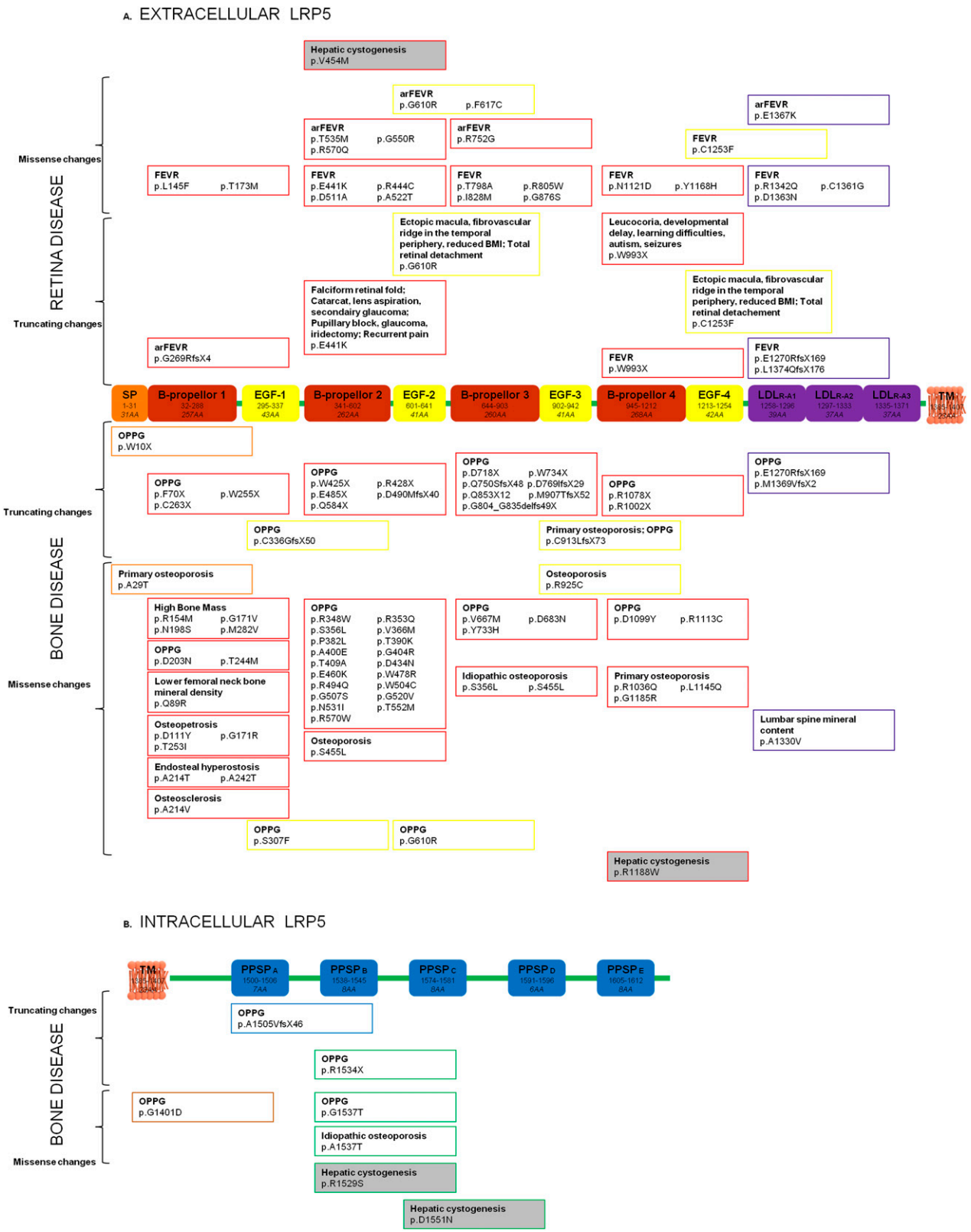

Fig. S3. Extracellular and intracellular *LRP5* mutations. This figure summarizes the location and number of all nonsense and missense mutations in the highly conserved *LRP5* gene resulting in a truncated or an amino acid change of the LRP5 protein. There are 88/117 (75%) nonsense and missense mutations identified in the *LRP5* gene causing multiple complex diseases: autosomal dominant and autosomal recessive retina or bone diseases. Hepatic or renal cystogenesis has not been observed in association with FEVR or with bone diseases. A considerable genetic locus heterogeneity in *LRP5* is present. Mutations in the *LRP5* gene are spread throughout the extracellular (*A*) and intracellular LRP5 protein domains (*B*). One exception are missense mutations in high bone mass disease patients, which are only located at the first β-propeller domain in LRP5. Remarkably, more mutations at the extracellular LRP5 domains were identified. This

Legend continued on following page

overview indicates that the relationship between a retina or bone phenotype for specific domains or protein change is not obvious (unclear), which could explain the distribution of the identified *LRP5* mutations in polycystic liver patients. In conclusion, we identified four missense mutations in three unrelated families and one singleton patient with severe hepatic cystogenesis. All *LRP5* mutations were predicted to be damaging or deleterious with profound structural effects on the LRP5 protein, especially the extracellular domains. We have not detected these variants in either DNA from healthy unrelated individuals from similar ancestry or assessed in the in-house data (1,300 individuals) and online sequence data (6,500 individuals from the ESP cohort; 1000 Genomes Project) (1, 2). We performed additional clinical and functional investigations to underline our findings. Protein domain information was derived from the MRS database; v6 (latest version); http://mrs.cmbi.ru.nl/m6/entry?db=sprot&id=lrp5_human&rq=lrp5_human (3); *LRP5* mutations were derived from a recent review by Nikopoulos et al. (4) and the Human Gene Mutation Database (www.biobase-international.com/hgmd) (5). Small indels (n = 2), deletions (n = 13), insertions (n = 4) and splice site (n = 8) mutations were not included in this figure.

1. National Institute of Environmental Health Sciences (2012) Environmental Genome Project Exome Variant Server. Available at http://evs.gs.washington.edu/niehsExome/. Accessed September 28, 2012.
2. Abecasis GR, et al.; 1000 Genomes Project Consortium (2010) A map of human genome variation from population-scale sequencing. *Nature* 467(7319):1061–1073.
3. Hekkelman ML, Vriend G (2005) MRS: A fast and compact retrieval system for biological data. *Nucleic Acids Res* 33(Web Server issue):W766–W769.
4. Nikopoulos K, et al. (2010) Overview of the mutation spectrum in familial exudative vitreoretinopathy and Norrie disease with identification of 21 novel variants in FZD4, LRP5, and NDP. *Hum Mutat* 31(6):656–666.
5. Stenson PD, et al. (2009) The Human Gene Mutation Database: 2008 update. *Genome Med* 1(1):13.

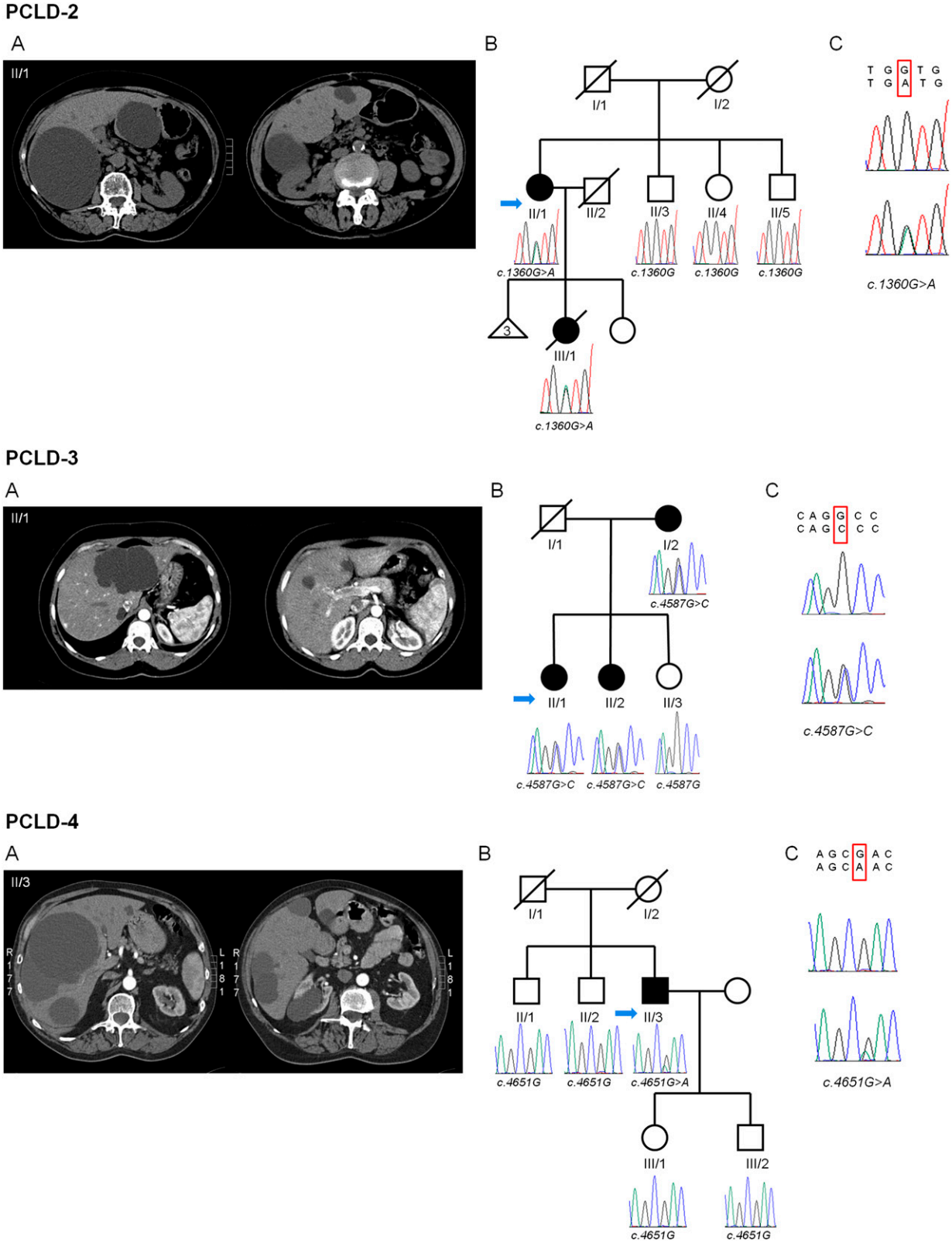

Fig. S4. CT scanning of the proband and pedigree of three additional PCLD families with a *LRP5* missense mutation. The *LRP5* mutation cosegregated with the disease phenotype in PCLD families 1, 2, and 3. All missense mutations were predicted to be pathogenic. For each family, (*A*) CT scanning of the proband (blue arrow in *B*) and (*B*) the pedigrees of family PCLD-2, PCLD-3, and PCLD-4. (*C*) Positions of the mutations are denoted according to the hg19 human reference genome (GRCh37) (1, 2). PCLD-2 family: *LRP5* g.68154128, *c.1360G* > *A*; p.V454M. PCLD-3 family: *LRP5* g.68216277; *c.4587G* > *C*; p.R1529S. PCLD-4 family: *LRP5* g.68216341; *c.4651G* > *A*; p.D1551N.

1. Kent WJ, et al. (2002) The human genome browser at UCSC. *Genome Res* 12:996–1006.
2. Meyer LR, et al. (2013) The UCSC Genome Browser database: Extensions and updates 2013. *Nucleic Acids Res* 41(Database issue):D64–D69.

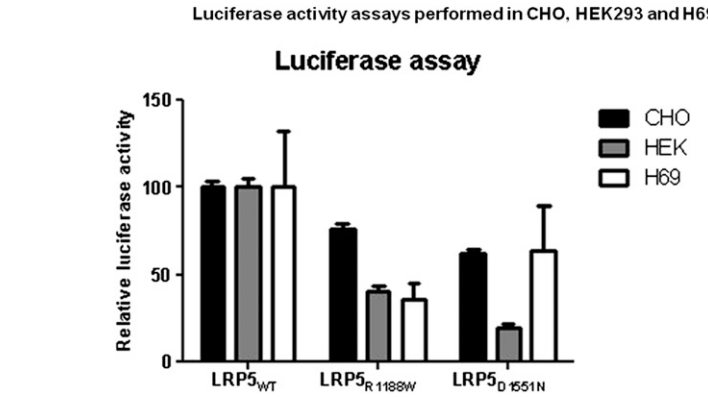

Fig. S5. Luciferase activity assays for $LRP5_{WT}$ and both mutant constructs $LRP5_{R1188W}$ and $LRP5_{D1551N}$ performed in CHO, HEK293, and H69 cells. Firefly luciferase activity was normalized to renilla luciferase activity by calculating the ratio. Wnt3a-induced signal activity was reduced in all cell systems compared with the $LRP5_{WT}$ ($P < 0.001$).

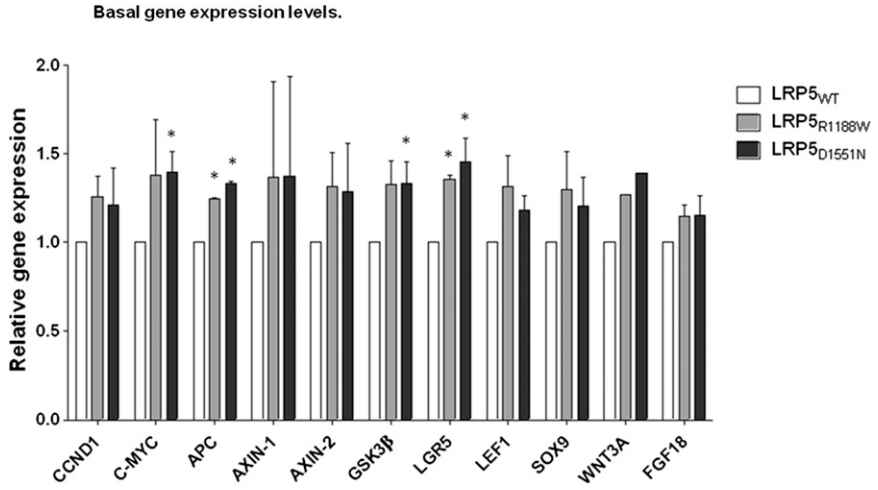

Fig. S6. Basal gene expression level genes involved in the canonical Wnt signaling pathway (for example). No Wnt3a was added to activate signaling. We corrected results for $LRP5_{WT}$ levels. *Significant increased expression levels. The *y* axis presents the relative gene expression level.

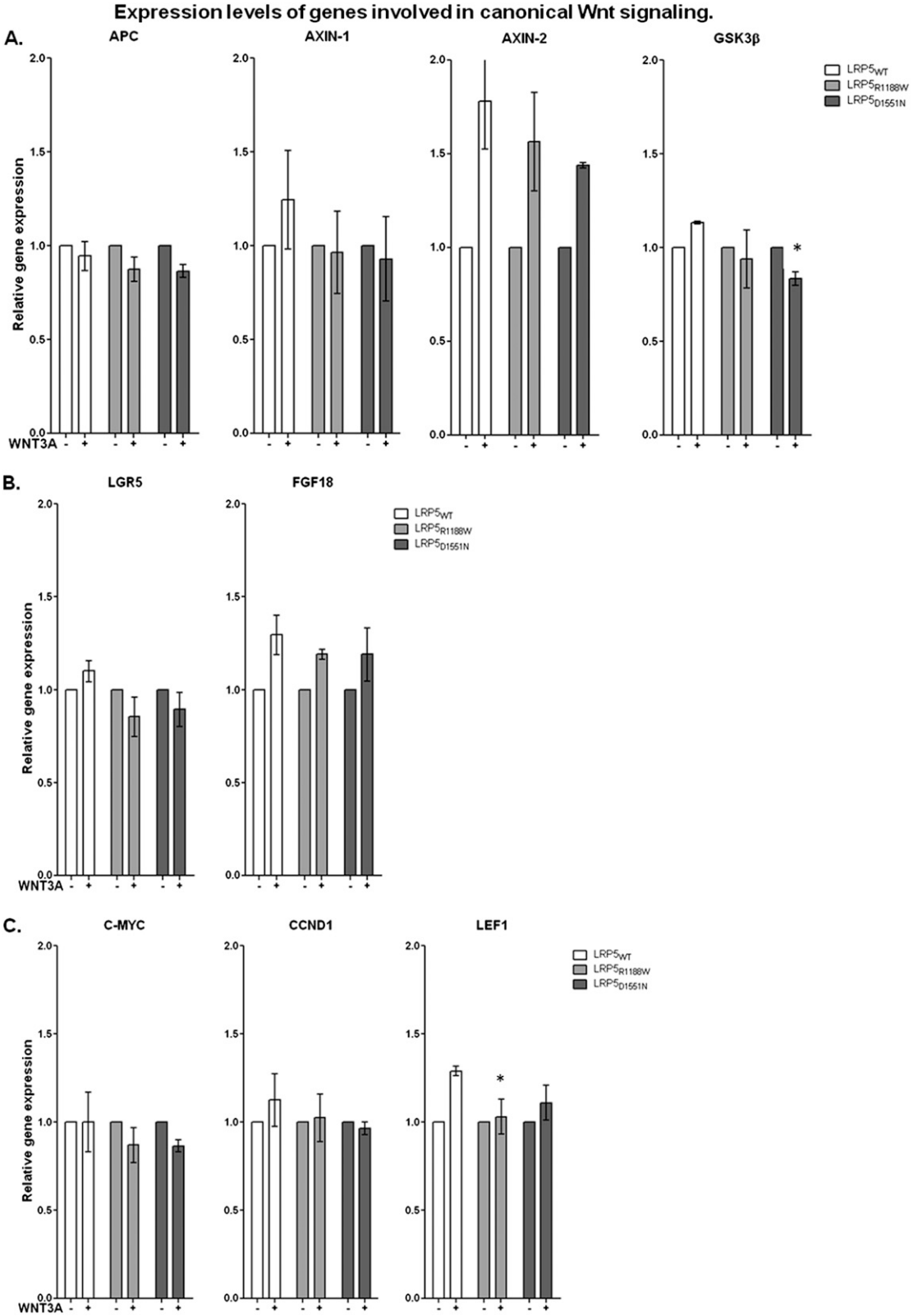

Fig. S7. (*A*) Gene expression levels of APC, AXIN-1, AXIN-2, and GSK3β involved in β-catenin degradation. (*B*) Expression levels of other target genes of the canonical Wnt signaling. (*C*) Expression levels of target genes at the nuclear end point of the canonical Wnt signaling pathway. In all panels, the first bar presents the unstimulated situation (basal gene expression levels). Expression levels of the second bar are the result of activation of the Wnt signaling by extracellular ligand Wnt3a. Activated gene expression levels are corrected for basal gene expression of the respective $LRP5_{WT}$, $LRP5_{R1188W}$, and $LRP5_{D1551N}$ constructs. *Significant decreased expression levels. The *y* axis presents the relative gene expression level.

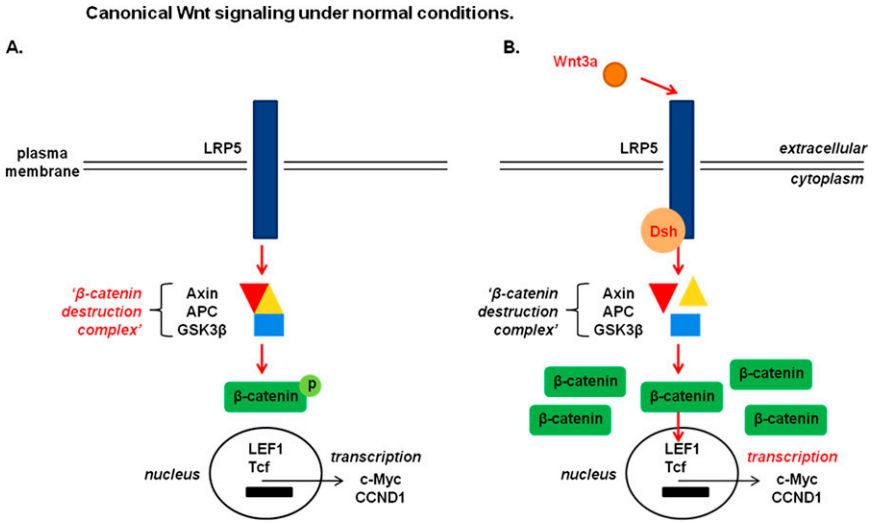

Fig. S8. Canonical Wnt signaling without an extracellular regulator (*A*) and activated with Wnt3a (*B*) under normal conditions. In red, the effects and signaling direction are indicated.

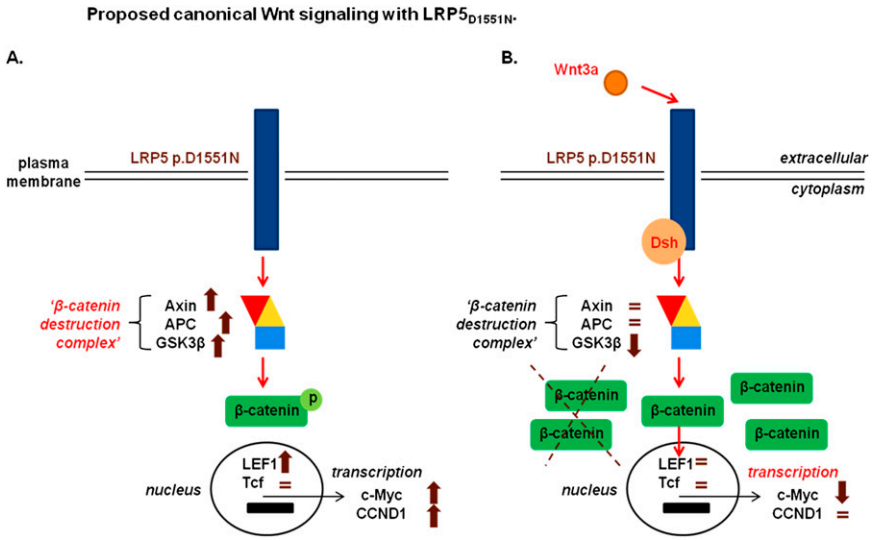

Fig. S9. Canonical Wnt signaling without an extracellular regulator (*A*) and activated with Wnt3a (*B*) in PCLD (*LRP5* mutation p.D1551N). Brown arrows indicate the altered expression levels of the involved target genes from our experiments.

Table S1. Summary of whole-exome sequencing performance in two probands of PCLD-1 family

Performance characteristics	III/18	II/18
Total mapped bases in regions	3.9G (79.0%)	2.8G (76.8%)
Total mapped bases near regions	0.41G (8.3%)	0.30G (8.0%)
Total mapped bases outside regions	0.62G (12.7%)	0.56G (15.2%)
Total reads	126M	108M
Total mapped reads	103M (81.6%)	80M (74.13%)
0 mismatches	58M	36M
Uniquely placed reads	85M	64M
Median target coverage	58.07x	41.70x
Percent targets covered ≥10×	83.9%	83.4%
Percent targets covered ≥20×	76.5%	74.4%

Table S2. Prioritization of private variants

Subsequent prioritization steps	III/18	II/18
Number of called private variants*	24,178	25,332
Exonic and canonical splice sites	11,705	12,083
Nonsynonymous and splice sites	5,743	6,004
Novel dbSNP v134 (1)	334	373
Absent in in-house database†	72	11
Shared variants‡	11	

*Private variant: A unique nucleotide change (on DNA level) derived from an individual in which exome sequencing was performed (in this study). These private variants may be benign or pathogenic depending on many factors (for example size/location/effect on amino acid or protein). Interesting candidate genes for unexplained disorders in patients may be unknown private variants not listed as a known SNP (polymorphism) or have a very low frequency in a population.

†In-house database: 1,300 whole-exome sequence data from individuals of predominantly European ancestry.

‡Shared variant: A private variant that is present in two affected individuals (in this study, affected members III/18 and II/18).

1. National Center for Biotechnology Information, National Library of Medicine (2012) Database of Single Nucleotide Polymorphisms (dbSNP). NCBI dbSNP Build 137. Available at www.ncbi.nlm.nih.gov/projects/SNP.

Table S3. Eleven private variants shared in both affected probands from PCLD-1 family

Chromosome	Position (hg19)	Reference	Variant	Gene name	Amino acid change	PhyloP	Variant in members with PCLD*	Variant in members with no PCLD
chr1	g.247769018	C	A	*OR2G3*	p.T44N	0.17	6/16	4/16
chr11	g.65633353	G	T	*MUS81*	p.G526V	5.181	9/16	15/16
chr11	g.68193580	C	T	*LRP5*	p.R1188W	0.016	16/16	0/16
chr11	g.99932087	G	A	*CNTN5*	p.R375H	3.051	8/16	3/16
chr12	g.13102792	T	C	*GPRC5D*	p.Y176C	5.247	6/16	7/16
chr15	g.31341712	C	A	*TRPM1*	p.V458L	5.479	8/16	7/16
chr15	g.43712642	A	T	*TP53BP1*	p.R1509E	0.791	8/16	4/16
chr16	g.71674378	T	A	*MARVELD3*	p.S227W	−0.534	11/16	8/16
chr6	g.129581891	A	G	*LAMA2*	p.Y711C	0.302	8/16	9/16
chrX	g.105190439	G	A	*NRK*	p.V1446M	2.433	7/16	4/16
chrX	g.149840060	C	T	*MTM1*	p.H602Y	4.244	6/16	2/16

*Eight members excluded during high-resolution melting curve analysis and direct Sanger sequencing (<40 y old and/or renal cystogenesis/no PCLD): II/13, III/22, III/26, IV/1, IV/2, IV/3, IV/4, and IV5.

Table S4. Clinical presentation of PCLD families included for genotype analysis

Inclusion (n = 40) PCLD-1	Sex	Age (y)	Liver phenotype (n = 16)	Kidney phenotype (n = 12)	Diagnosis (PCLD n = 16; renal cyst(s) n = 3)	*LRP5* mutation (n = 22)
>40 y						
I/1	F	42*	NA	NA	NA	NA
I/2	M	70*	NA	NA	NA	NA
II/1[†]	F	81*	Y	Y	PCLD	NA
II/3	F	47*	NA	NA	NA	NA
II/4	F	85	N	N	No PCLD	Normal
II/5	F	82*	NA	NA	NA	NA
II/7	F	72*	NA	NA	NA	NA
II/9	F	80	Y	N	PCLD	p.R1188W
II/11	F	79*	NA	NA	NA	NA
II/13[‡]	M	78	N	Y	Renal cysts	p.R1188W
II/15	M	56*	NA	NA	NA	NA
II/16	F	76*	NA	NA	NA	NA
II/18[§]	F	72	Y	Y	PCLD	p.R1188W
II/20	F	57*	NA	NA	NA	NA
III/1	F	58	Y	Y	PCLD	p.R1188W
III/3	F	56	Y	Y	PCLD	p.R1188W
III/5	F	55	Y	Y	PCLD	p.R1188W
III/6	M	54*	Y	N	PCLD	p.R1188W
III/7	F	52	N	N	No PCLD	Normal
III/9[¶]	M	51	Y	Y	PCLD/ADPKD	p.R1188W
III/10	F	50	N	N	No PCLD	Normal
III/11	M	47	N	N	No PCLD	Normal
III/12	M	46	N	N	No PCLD	Normal
III/13	M	42	Y	Y	PCLD	p.R1188W
III/14	F	44	Y	N	PCLD	p.R1188W
III/15	M	58	N	N	No PCLD	Normal
III/16	M	54	N	N	No PCLD	Normal
III/17	M	48	N	N	No PCLD	Normal
III/18[‖]	F	53	Y	N	PCLD	p.R1188W
III/19	F	51	Y	N	PCLD	p.R1188W
III/20	F	48	N	N	No PCLD	Normal
III/21	F	52	N	N	No PCLD	Normal
III/22	M	49	N	N	No PCLD	p.R1188W
III/23	M	42	N	N	No PCLD	Normal
III/24	M	42	N	N	No PCLD	Normal
III/25	F	51	Y	N	PCLD	p.R1188W
III/26	M	50	N	Y	Renal cysts	p.R1188W
III/27	F	44	Y	Y	PCLD	p.R1188W
III/28	F	43	Y	N	PCLD	p.R1188W
III/29	M	51	Y	Y	PCLD	p.R1188W
III/30	F	47	Y	Y	PCLD	p.R1188W
III/31	F	46	N	N	No PCLD	Normal
III/32	F	48	N	N	No PCLD	Normal
III/33	M	47	N	N	No PCLD	Normal
III/34	M	45	N	N	No PCLD	Normal
<40 y						
IV/1	F	36	N	N	Indeterminate	Normal
IV/2	M	34	N	N	Indeterminate	Normal
IV/3	F	33	N	N	Indeterminate	p.R1188W
IV/4	M	30	N	N	Indeterminate	p.R1188W
IV/5	M	26	N	Y	Renal cyst	p.R1188W

Inclusion (n = 14)	Sex	Age	Liver phenotype (n = 6)	Kidney phenotype (n = 2)	Diagnosis (PCLD n = 6; ADPKD n = 0)	LRP5 mutation (n = 6)
PCLD-2						
I/1	M	75*	NA	NA	NA	NA
I/2	F	79*	NA	NA	NA	NA
II/1 (index)	F	86	Y	N	PCLD	p.V454M
II/3	M	83	N	N	No PCLD	Normal
II/4	F	77	N	N	No PCLD	Normal
II/5	M	67	N	N	No PCLD	Normal

Table S4. Cont.

Inclusion (n = 40) PCLD-1	Sex	Age (y)	Liver phenotype (n = 16)	Kidney phenotype (n = 12)	Diagnosis (PCLD n = 16; renal cyst(s) n = 3)	*LRP5* mutation (n = 22)
III/1	F	49*	Y	Y (4 small cysts)	PCLD	p.V454M
PCLD-3						
I/1	M	67*	NA	NA	NA	NA
I/2	F	71	Y	N	PCLD	p.R1529S
II/1	F	48	Y	N	PCLD	p.R1529S
II/2 (index)	F	43	Y	N	PCLD	p.R1529S
II/3	F	40	N	N	No PCLD	Normal
PCLD-4						
I/1	M	73*	NA	NA	NA	NA
I/2	F	82*	NA	NA	NA	NA
II/1	M	70	N	N	No PCLD	Normal
II/2	M	67	N	N	No PCLD	Normal
II/3 (index)	M	65	Y	Y (3 cysts)	PCLD	p.D1551N
III/1	F	38	N	N	No PCLD	Normal
III/2	M	35	N	N	No PCLD	Normal

We performed abdominal ultrasound screening of the liver and kidneys in 39 members of proband III/18 from the PCLD-1 family. Ultrasound images of liver and kidneys were acquired using a 3.6-MHz general purpose clinical echo system (Acuson ×150; Siemens AG) equipped with a curved linear array transducer. Presence or absence of cysts was carefully noted in all living relatives. For almost all deceased relatives, DNA from blood or tissue and radiological imaging was not available. An abdominal CT scan for only one diseased patient (II/1) was present and showed a severe polycystic liver, but no DNA was available. Member III/6 died after inclusion during the research process. We restricted our inclusion to the five oldest members from the fourth generation of PCLD-1 family because of the late onset of hepatic cystogenesis (>40 y), especially in males. These members are recognized as individuals at risk for PCLD, which is associated with age-dependent occurrence and development of hepatic cysts (1). Individual IV/5 was known with a large dominant renal cyst and his father (III/9) showed a severe polycystic liver and multiple cysts in both kidneys. Finally, 40 members were included for genotype analysis (excluding patient II/1). Three males (II/13, III/22, and III/26) were categorized as "No PCLD" because they did not fully met the Reynolds criteria for PCLD, even after reevaluation in II/13 and III/26 (*SI Text*) (1). Two males had bilateral renal cysts (and splenic cysts in individual II/13) with a positive family history of PCLD. All three members possessed the *LRP5 c.3562C > T* (p.R1188W) missense mutation. The mild or indeterminate phenotype in these members can be explained by the age-dependent factor for hepatic cyst formation, but even more by the predominant hepatic cystogenesis development in females and an evident known incomplete penetrance of ∼80% in PCLD (2–4). There was no renal disease nor renal failure present in this PCLD family; however, 12 members possessed several renal cysts. Only patient III/9 was affected with numerous cysts in both kidneys closely associated to the ADPKD criteria (5, 6). F, female; M, male; N, no cysts present; NA, no data available; Y, yes, cysts present.

*Deceased and age of death.

†Radiological data resources.

‡Splenic cysts.

§Exome sequencing performance 2 in individual II/18.

¶PCLD phenotype correlates with the ADPKD Ravine criteria (5, 6).

||Exome sequencing performance 1 in individual III/18.

1. Reynolds DM, et al. (2000) Identification of a locus for autosomal dominant polycystic liver disease, on chromosome 19p13.2-13.1. *Am J Hum Genet* 67(6):1598–1604.
2. Chapman AB (2003) Cystic disease in women: Clinical characteristics and medical management. *Adv Ren Replace Ther* 10(1):24–30.
3. Van Keimpema L, et al. (2011) Patients with isolated polycystic liver disease referred to liver centres: Clinical characterization of 137 cases. *Liver Int* 31(1):92–98.
4. Gabow PA, et al. (1990) Risk factors for the development of hepatic cysts in autosomal dominant polycystic kidney disease. *Hepatology* 11(6):1033–1037.
5. Ravine D, et al. (1994) Evaluation of ultrasonographic diagnostic criteria for autosomal dominant polycystic kidney disease 1. *Lancet* 343(8901):824–827.
6. Pei Y, et al. (2009) Unified criteria for ultrasonographic diagnosis of ADPKD. *J Am Soc Nephrol* 20(1):205–212.

Table S5. Templates for homology models of LRP5 protein domains

Domain in LRP5	PDB ID code	LRP5 identity (%)	Reference
First WD40	3SOV	73	(1)
Second WD40	3S94	79	(2)
Third WD40	4A0P	80	(3)
Fourth WD40	4A0P	65	(3)

We identified four unique *LRP5* variants of which two are located extracellularly and two are located intracellularly. The LRP5 protein structure was created by using a LRP6 template as start homology model and reconstruction by YASARA&WHAT-IF Twinset (4). PDB files for homology modeling were available for four WD40 domains (β-propeller subdomains). Two *LRP5* variants are located at the second and fourth WD40 domains, respectively (Fig. 1). Separate models for these domains and the mutations were visualized and analyzed using YASARA.

1. Bourhis E, et al. (2011) Wnt antagonists bind through a short peptide to the first β-propeller domain of LRP5/6. *Structure* 19(10):1433–1442.
2. Cheng Z, et al. (2011) Crystal structures of the extracellular domain of LRP6 and its complex with DKK1. *Nat Struct Mol Biol* 18(11):1204–1210.
3. Chen S, et al. (2011) Structural and functional studies of LRP6 ectodomain reveal a platform for Wnt signaling. *Dev Cell* 21(5):848–861.
4. Krieger E, et al. (2009) Improving physical realism, stereochemistry, and side-chain accuracy in homology modeling: Four approaches that performed well in CASP8. *Proteins* 77(Suppl 9): 114–122.